

Division - Soil in Space and Time | Commission - Soil Genesis and Morphology

Epi and endosaturation affecting redoximorphic features and pedogenesis in subtropical soils with high textural contrast developed from sedimentary rocks

Jaime Antonio de Almeida^{(1)*}  and Pablo Grahl dos Santos⁽²⁾ ⁽¹⁾ Universidade do Estado de Santa Catarina, Centro de Ciências Agroveterinárias, Departamento de Solos e Recursos Naturais, Lages, Santa Catarina, Brasil.⁽²⁾ Universidade do Estado de Santa Catarina, Centro de Ciências Agroveterinárias, Programa de Pós-Graduação em Ciência do Solo, Lages, Santa Catarina, Brasil.

ABSTRACT: Soils in the Depressão Central and Campanha Gaúcha in Rio Grande do Sul State, Brazil, developed from sedimentary rocks are mainly Alfisols (*Luvissoles*, *Planossolos* and *Plintossolos*) and Ultisols (*Argissolos*) with high textural contrast between A and/or E horizons and clayey B horizons. Red Ultisols dominate in well-drained areas in the summit. But many soils present redoximorphic features on the backslope and footslope, with mottled and/or nodules similar to plinthite due to the oscillating of the water table above the rock or poorly permeable saprolite. Identifying morphological features, mineralogical and chemical properties, and parent material differences are essential to identify the main processes responsible for their genesis. Knowledge of the relative distribution of different forms of iron in the soil is also of particular interest when interpreting pedogenesis. This study aimed to evaluate the main process responsible for the high textural contrast in soils developed from different sedimentary lithologies, and how the redoximorphic features observed in some soils may be related to genesis of plinthites and ferrolysis processes. The study area is located in the hydrographic basin of Rio Santa Maria, in the city of Rosário do Sul - RS, Brazil (30° 15' 28" S and 54° 54' 50" W), average altitude of 132 m and Cfa-type climate. Topolithosequences were defined based on soils developed from lithologies of Piramboia and Sanga-do-Cabral geological formations, by choosing soil profiles according to the source material, variations in relief, altitude and hydrological conditions. Morphological descriptions, particle size determinations, chemical analysis, mineralogy of the clay fraction by XRD analysis, determination of the main forms of iron, tests to identify plinthite were performed. Argiluviation, ferrolysis and plinthization were the most active processes identified in the genesis of most studied soils. The high textural contrast on these soils was not solely due to clay illuviation processes but also ferrolysis and lithological discontinuities in some soils, indicating polygenetic origin. Redoximorphic features in most soil revealed that iron segregation in most soils occurs like mottles and not plinthite, since they did not remain aggregated after the various wetting and drying cycles.

Keywords: pedogenesis, iron oxides, ferrolysis, plinthite.*** Corresponding author:**

E-mail: jaime.almeida@udesc.br

Received: May 04, 2021**Approved:** August 26, 2021

How to cite: Almeida JA and Santos PG. Epi and endosaturation affecting redoximorphic features and pedogenesis in subtropical soils with high textural contrast developed from sedimentary rocks. Rev Bras Cienc Solo. 2021;45:e0210044.

<https://doi.org/10.36783/18069657rbc20210044>

Editors: José Miguel Reichert  and Alberto Vasconcellos Inda Júnior .

Copyright: This is an open-access article distributed under the terms of the Creative Commons Attribution License, which permits unrestricted use, distribution, and reproduction in any medium, provided that the original author and source are credited.



INTRODUCTION

Gondwanic sedimentary rocks of the Pirambóia and Sanga-do-Cabral formations predominate in the Ibicuí river - Negro river depression (CPRM, 2006) of Rio Grande do Sul State, Brazil, whose lithologies constitute the substrate of several soil types, among which Ultisols and Alfisols, with or without plinthite, and with high textural contrast stand out between horizons A and B. There is a standard distribution for the soils in the landscape. It is relatively simple, with red Ultisols occupying the highest shares, where they develop on sandstones. The Alfisols and some Ultisols occupy the lower thirds of the slopes with long pendants and smooth undulating relief, usually originated from siltstones and mudstones with intense mottles and features similar to plinthite at the base of profiles. The soils with plinthite usually occur at the base of the steepest slopes, due to vertical drainage restrictions caused by poorly permeable siltstones and the accumulation of Fe compounds from the lateral subsurface transport (Brasil, 1973; IBGE, 1986; Streck et al., 2008).

High textural contrast is a common feature in soils of this region, characterized by the strong increase of clay in-depth and/or abrupt textural change (Almeida, 2017). Textural contrast in soils is usually due to clay illuviation processes (Soil Survey Staff, 1999) or lithologic discontinuity caused by the deposition of coarser sedimentary material on a pre-existing soil (Schaetzl, 1998; Michelon et al., 2010). However, although many of these soils present morphological features and properties indicative of argilluviation processes (Kämpf and Curi, 2012), the hypothesis that high textural contrast can also be formed by the contribution of processes such as ferrollysis (Brinkman, 1970, 1977, 1979; Jimenez-Rueda and Demattê, 1988; Andrade, 1990; Almeida et al., 1997; Oliveira Junior et al., 2017) is not discarded.

Many soils in the depression of the Ibicuí-Negro rivers are moderate to imperfectly drained, even in undulating relief, and present redoximorphic features (Vepraskas, 2015) from the top of the B horizon to the contact with the rock or saprolite. The colors become more grayish in depth due to the drainage restriction caused by the presence of pellic rock saprolite, forming iron depletion zones associated with the presence of mottled and variegated patterns at the profile base (Almeida, 2017). This raises questions about the correct characterization of this material since part of the iron segregations is very similar to plinthite, but it is also similar to the fragments of unaltered material from the underlying rock or reddish saprolite.

The relative distribution of iron forms is of interest when interpreting pedogenesis, when evaluating weathering conditions and intensity, when understanding the soil's physical and chemical behavior, and when classifying soils (Inda Jr and Kämpf, 2003). Iron oxides in soils are mostly composed of new products derived from the changes in sediments and soil materials (Pereira and Anjos, 1999), meaning that the origin is conditioned by the environment, where concentrations are closely related to the type of source material, weathering intensity, and pedogenetic processes of accumulation or removal (Kämpf and Curi, 2000).

This study aimed to evaluate the main process responsible for the high textural contrast in soils developed from different sedimentary lithologies and how the redoximorphic features observed in some soils may be related to genesis of plinthites and ferrollysis processes.

MATERIALS AND METHODS

The study area is located at the Physiographic Region of the Campanha Gaúcha, at the Geomorphological Province of the Central Depression, Geomorphological Province of the Central Depression of Ibicuí river-Rio Negro (Justus et al., 1986), extending from the city

of Rosário do Sul to Santana do Livramento - Rio Grande do Sul state, Brazil (Figure 1). The municipality of Rosário do Sul, main location of the studied soils, is located at 30° 15' 28" south latitude and 54° 54' 50" west longitude, with an average altitude of 132 m. Climate, according to Köppen's classification system (Köppen and Geiger, 1928) is temperate, the subtropical humid type, with warm summers and cold winters (Cfa), and a median annual rainfall rate between 1300 to 1600 mm (PMRS, 2005).

The choice of sampling sites (soil profiles) considered various soilscape elements, the different types of source material, variations in relief and altitude, rock outcrops, soil color, accessibility (roads) and road cuts available, with the aid of geotechnologies, by means of real-time spatial positioning in a GIS environment on the cartographic base with a GPS

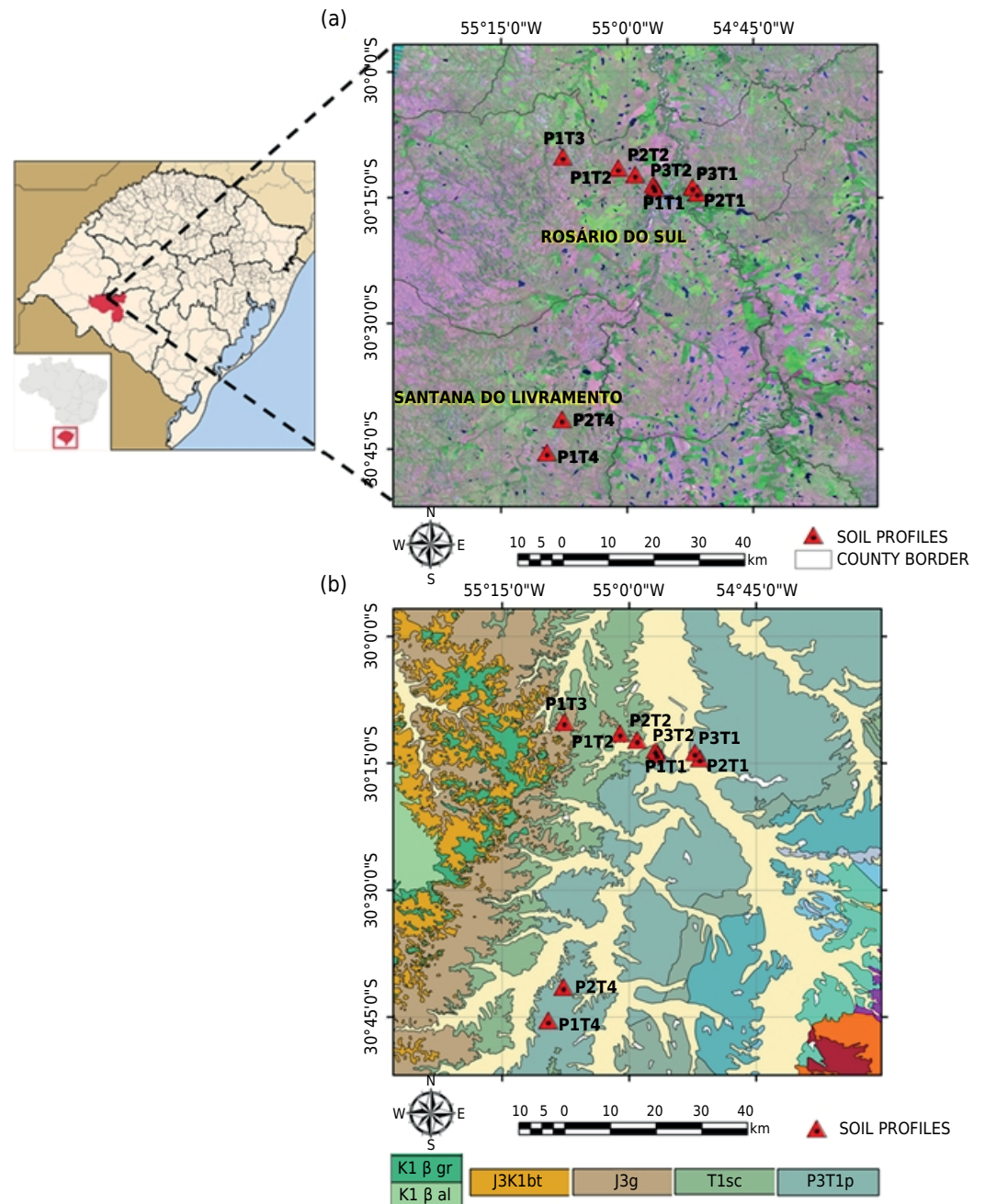


Figure 1. Image chart with the geographic location of the study area and soil profiles - Municipality of Rosário do Sul and Santana do Livramento/RS (Landsat Image 5 Thematic Mapper - Composition 5R4G3B / Datum SAD69 - Indicated Scale) (a); Simplified geological map of part of the southwest region of the state of Rio Grande do Sul (b). Main Formations - P3T1p: Pirambóia Formation; T1sc: Sanga-do-Cabral Formation; J3g: Guará Formation; J3K1bt: Botucatu Formation; K1β: Serra Geral Formation (scale indicated).

navigation receiver. Therefore, a traditional toposequence was not characterized, but different soils formed from different lithologies in different segments of the landscape (topolithosequence). The elevation map with the altitude distribution (hypsothetic levels) in vertical equidistant intervals, the layout and the topographic profile maps of the topolithosequences are shown in figure 2.

Profiles P1T1, P2T1, P3T1, P1T4, and P2T4 belong to the Pirambóia formation, profiles P1T2, P2T2, and P3T2 belong to the Sanga-do-Cabral formation (Figure 1b). The Pirambóia formation comprises medium to fine sandstone, with well-developed lenticular geometry, deposited in a continental, wind environment with fluvial intercalations, where layers of siltstones can also occur, interspersed with the sandstones. The Sanga-do-Cabral formation belongs to the Rosário do Sul group, and is characterized by subarkosis and arkosis, elongated tabular or lenticular bodies, constituted by a gap and intraformational conglomerate, siltstone and mudstones, deposited in a continental, fluvial interlaced environment, containing fragments of fossil vertebrates (CPRM, 2006). Soares et al. (2008) identified two units within the Sanga-do-Cabral formation. The upper portion consisting of poorly selected red and pink thin to thick sandstones, interpreted as fluvial deposits. In the lower portion, quartzite red sandstones, with crossed-bedding, which are interspersed with reddish sandstones, thin to medium granulometry, clayey matrix and sub-horizontal stratification, interpreted as wind-caused. According to Andreis et al. (1980) the upper sandstones present laminated siltstone and sandstone intersperses with incipient parallel flat stratifications, and carbonate concretions.

After choosing the soil profiles, a general and morphological description was carried out according to Santos et al. (2005). Subsequently, in each profile sub-horizons, a deformed sample was collected for chemical, physical and mineralogical characterization. After air drying, clod breaking, grinding, and sieving the samples using 2 mm mesh, the coarse fractions were separated, and the air-dried fine earth (ADFE) was stored. The ADFE was

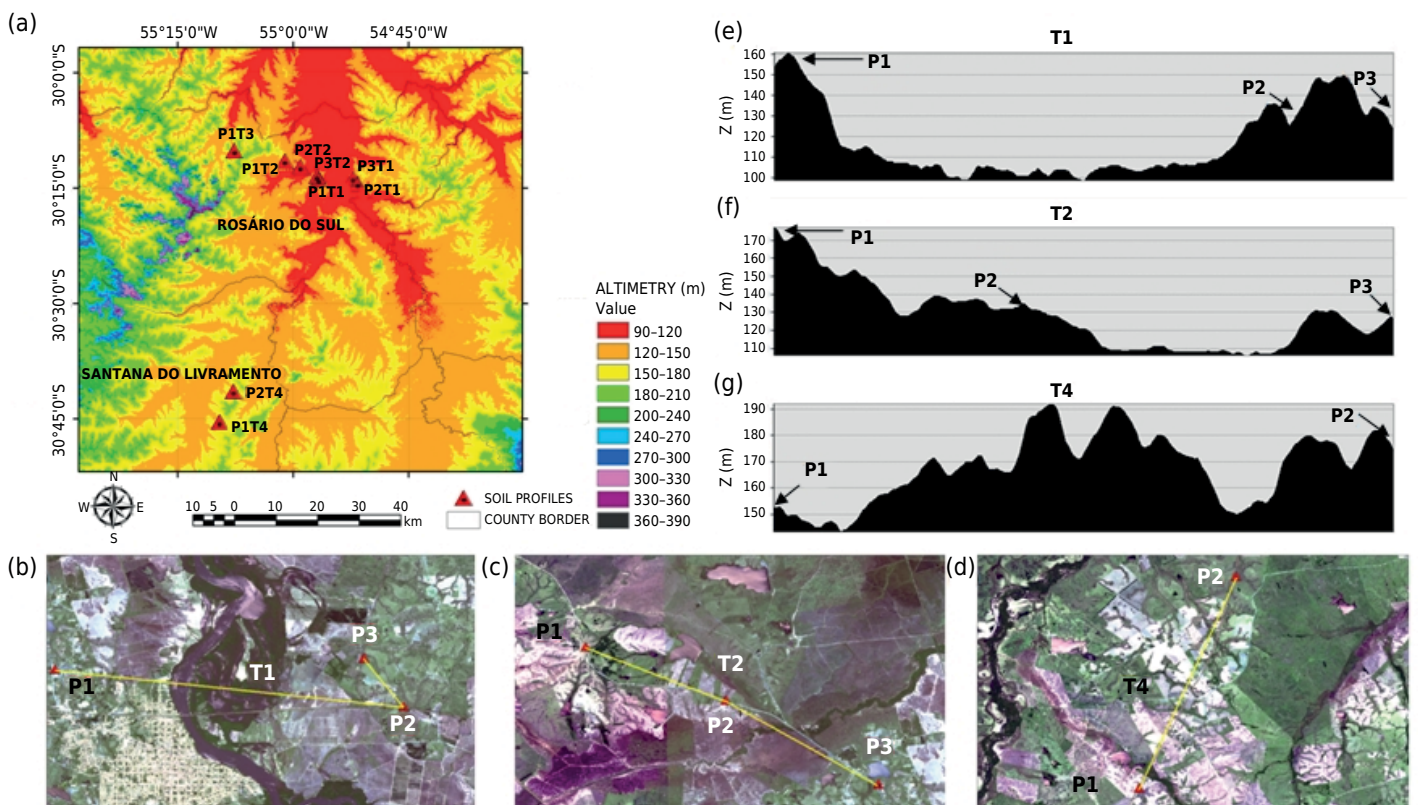


Figure 2. (a) Altimetric map of the region (*Datum* SAD69 - scale indicated); Tracing of the topolithosequences: T1 (P1, P2 and P3 profiles) (b), T2 (P1, P2 and P3 profiles) (c) and T4 (P1 and P2 profiles) (d) (RapidEye Image Composition 3R2G1B - without scale); topographic profile map of the topolithosequences T1 (e), T2 (f) and T4 (g) built from the MDE (without scale).

submitted to granulometric and basic chemical analyzes according to the methods described in Tedesco et al. (1995) and Claessen (1997).

Active acidity (pH in H₂O and KCl 1 mol L⁻¹ with a soil:solution ratio of 1:1) was determined by potentiometry using a pH meter. Organic carbon (C org) was determined using the Walkley-Black method through its oxidation with the dichromate anion in an acid medium and REDOX titration with an iron sulfate solution, in the presence of a ferroin indicator. Exchangeable potassium and sodium contents were determined using the double acid extractor method (Mehlich-1) with readings in a flame photometer. Calcium and magnesium were extracted with KCl 1 mol L⁻¹ and determined in an atomic absorption spectrophotometer. Exchangeable aluminum was obtained by neutralization titration with NaOH 0.0125 mol L⁻¹ in the same extract as above. Potential acidity [H+Al] was obtained with a 0.5 mol L⁻¹ calcium acetate extractor buffered to pH 7 and titration with NaOH 0.02 mol L⁻¹. The sum of bases (S), the cation exchange capacity at pH 7 (T) and base saturation (V) were calculated, according to the following expressions: $S = Ca^{2+} + Mg^{2+} + K^+ + Na^{2+}$; $CTC\ pH7\ (T) = S + [H+Al]$; $V_{\%} = (S / T) \times 100$.

Contents of Fe₂O₃ and Al₂O₃ were quantified in the extracts of the sulfuric attack on the ADFE, according to Claessen (1997) and the ammonium acid oxalate described in Schwertmann (1964). The procedure described in Mehra and Jackson (1960), adapted by van Reeuwijk (2002) for the determination of DCB iron (sodium dithionite-citrate-bicarbonate) was also applied. The contents were quantified by atomic absorption spectrophotometer. The following ratios were calculated: Al_s/Fe_s; Al_o/Fe_o; Fe_o/Fe_s; Fe_d/Fe_s; and Fe_o/Fe_d, where: Al_s is aluminum sulfuric attack; Fe_s is iron sulfuric attack; Al_o is aluminum oxalate; Fe_o is iron oxalate; and Fe_d is DCB iron.

Total contents of iron, silicon and aluminum in the clay fraction, expressed in the form of oxides, was also carried out using the XRF (X-ray fluorescence) technique, using a compact X-ray dispersible energy spectrometer (XDE) PANalytical's Epsilon 3 model. The Ki and Kr indexes were calculated from the XRF results of the clay fraction for the following molecular ratio: $Ki_{XRF} = 1.7 \times (\% SiO_2 / \% Al_2O_3)$ and $Kr_{XRF} = 1.7 \times \{ \% SiO_2 / [\% Al_2O_3 + (0.6325 \times \% Fe_2O_3)] \}$.

Granulometric analysis was determined by the simplified densimeter method (Bouyoucus, 1962), the clay fraction being determined after dispersing the samples in H₂O - natural clay (An), and with NaOH 1 mol L⁻¹ or Calgon (sodium hexametaphosphate and anhydrous sodium carbonate) - total clay (A_T). The sand was quantified by weighing after sieving and drying it in an oven. The clay fraction was later separated from the silt using sedimentation, in accordance with Stokes' law, and stored in dry and in suspended form, for differential chemical and thermal treatments meant used in mineralogical analysis.

Sand was fractioned into classes by sieving (dry mechanical agitation) in a sieve shaker (rot-up). The sub-fractions of the clay particles were determined using a Mastersizer 2000 laser granulometer equipped with the accessory Hydro 2000MU from Malvern Instruments, being grouped in the following classes: coarse clay (2 to 1 μm) and fine clay (<1 μm).

Part of the clay fraction samples was subjected to saturation with potassium chloride (KCl 1 mol L⁻¹), and another to magnesium chloride solution (MgCl₂ 0.5 mol L⁻¹) Oriented clay blades were made after removing the excess salts, using the following treatments: saturated with K and Mg and read at room temperature (K25 and Mg25); saturated with Mg and solvated with ethylene glycol (Mg+EG) and saturated with K and then heated to 100, 350 and 550 °C (K100, K350 and K550).

Mineralogical characterization of the clay fraction was reached by XRD, using an automated Philips PW 3710 model X-ray diffractometer, equipped with a copper anode, vertical goniometer with a θ/2θ compensation angle, and a graphite monochromator, with an angular variation from 4 to 40° 2θ. The angular velocity was 0.02° 2θ/s, in step mode, with a time of 1s of reading per step. The results were interpreted based on the interplanar

spacing (d) and on the behavior of the diffraction reflexes, according to Brindley and Brown (1980), Whittig and Allardice (1986), and Resende et al. (2005), using tools from the APD (Automatic Powder Diffraction) and X'PERT HIGHSCORE PLUS programs, allowing the identification and semi-quantification of clay minerals.

Soil profile horizons samples that showed mottles and/or reddish nodules were selected and subjected to alternating cycles of moistening and drying in a protected environment to diagnose the presence of plinthite according to the methodology proposed by Jacomine et al. (2010). Profile samples that presented horizons with gray and reddish alteration spots and/or variegated coloring were subjected to manual physical separation by scraping the segregations of the soil matrix, with subsequent performance of chemical and mineralogical analyzes. The profiles were taxonomically classified according to the Brazilian Soil Classification System (Santos et al., 2018) and Soil Taxonomy (Soil Survey Staff, 2014).

RESULTS

Morphological data of the soil profiles, analytical results for chemical and physical characterization, and taxonomic classification of the soils are shown in tables 1 and 2. The general description of these soils and the complete analytical data can be consulted in Santos (2015). The morphological features of soil profiles studied, and a general view of them are shown in figure 3.

Profiles P1T1 and P2T4, both located at the top of elevations in gently undulating relief, are well-drained red Ultisols, with uniform reddish coloration and without mottles or plinthite. They were developed on the sandstone strata of the Pirambóia formation. Profiles P1T1 and P2T4 occur on slopes of 5 and 8 % and altitudes of 140 and 165 m, respectively.

The P2T1 is located in the lower third of the slope, in an undulating relief, with a 10 % declivity, developed on siltstone strata of the Pirambóia formation, at an altitude of 125 m. It is a moderately to imperfectly drained profile, with reddish and reddish brown mottles scattered throughout the upper portion of the B horizon, whose matrix presents brownish colors. On the 2BC horizon, the mottled are similar to plinthite and are dispersed in a grayer matrix with iron depletion, resulting from the dissolution of iron compounds by temporary reduction processes.

The P3T1 is moderately drained, located in the lower third of the slope with 15 % of declivity, whose slope is close and directed to the extensive floodplain of the Santa Maria River. It is developed on fine sandstones and siltstones from the Pirambóia formation, in undulating relief, at an altitude slightly higher (145 m) than the previous profile. An intense amount of mottling (or plinthite) is prominent and distinct in Btf2 and Btf3 interspersed with grayish spots in a yellow matrix. Manganese oxide depositions were observed on the horizontal and vertical faces of the prismatic aggregates. In Btf3, there are also gray spots in a matrix with a sandier texture, indicating possible ferrollysis processes. At the base of the profile, there are irregular, millimetric and some centimetric nodules of petroplinthite.

In toposequence 2, the profile at the highest altitude is P1T2, located at 172 m at the top of the elevation, in the transition zone to the backslope, with 10 % slope. It is a moderately drained profile, developed from sandstones and siltstones from the Sanga do Cabral formation, with a predominance of brownish colors in the matrix of the B horizon, but with some mottles along the B horizon.

The P2T2 is located in a half slope position, close to the previous profile and occurs at an altitude of 124 m, with a slope of 15 %. It is a shallow profile, developed on thin siltstone strata with carbonate cementation, being moderately drained. It has few



Figure 3. Soil profiles and landscape of occurrence: (a1 and a2) P1T1; (b1 and b2) P2T1; (c1 and c2) P3T1; (d1 and d2) P1T2; (e1 and e2) P2T2; (f1 and f2) P3T2; (g1 and g2) P1T4; and (h1 and h2) P2T4.

mottles and secondary calcium carbonate concretions in the Bt and Cr horizon, but no plinthite.

The P3T2 is located close to P2T2, but in another stream, at an altitude of 115 m, in the lower third of the slope, still developed on sedimentary strata of the Sanga do Cabral formation. It is developed from siltstones, with a sandy material on the surface horizon, probably originating from the alteration of sandstones of the adjacent Pirambóia formation, which are underneath the Sanga do Cabral formation. The reddish mottles, with millimeter

Table 1. Morphological characterization of the soil in horizons of the studied profiles

Horiz	Color (wet)		Structure			Consistency			Transition	
	Munsell	Degree ⁽¹⁾	Size ⁽²⁾	Type ⁽³⁾	Dry ⁽⁴⁾	Humid ⁽⁵⁾	Wet ⁽⁶⁾	Shape ⁽⁷⁾	Sharpness ⁽⁸⁾	
P1T1: Arenic Kanhapludults (PVD-Argissolo Vermelho Distrófico espessarênico abruptico)										
A1	7.5YR 3/4	we	sm & md	sub & ang.bl	s.hd	v.fri	n.plas & n.sti	pla	cl	
A2	7.5YR 3/3	we	sm & md	sub & ang.bl	hd	fri	n.plas & n.sti	pla	grad	
AE	7.5YR 4/4	we	sm & md	sub.bl	sof	v.fri to lo	n.plas & n.sti	wav	grad	
E	7.5YR 4/6	we	sm	sub.bl	sof	lo to v.fri	n.plas to s.plas & n.sti	pla	abrp	
Bt1	2.5YR 3/4	mod	md & sm	sub.bl	v.hd	v.fri to fri	v.plas & s.sti to sti	pla	cl	
Bt2	2.5YR 3/6	str	md	ang & sub.bl	v.hd to e.hd	fri	plas & peg to v.sti	pla	cl	
Bt3	2.5YR 3/6	str	md & lar	ang & sub.bl	e.hd	fri to fir	plas & sti	pla	grad	
BC	2.5YR 2.5/4	we to mod	md & lar	ang.bl	v.hd	v.fri to fri	s.plas to plas & sti	pla	grad	
P2T1: Oxyaquic Hapludults (PBACva-Argissolo Bruno-Acinzentado Ta Alumínico abruptico endorredóxico)										
A1	10YR 3/2	we	sm	gran & sg	sof	v.fri	n.plas & n.sti	pla	grad	
A2	10YR 2/2	we	md	sub & ang.bl	s.hd	fri	n.plas & n.sti	pla	cl	
2BA	7.5YR 3/2	mod	md & sm	sub.bl	hd	fri to fir	plas & peg	pla	grad	
2Bt	7.5YR 4/4 e 2.5YR 4/7	mod	lar & md	sub & ang.bl	e.hd	fir	s.plas to plas & s.sti	wav	grad	
2BC	7.5YR 4/2 and 2.5YR 3/6	we we	lar md & lar	prism ang & sub.bl	v.hd	fri	s.plas & sti	wav	grad	
P3T1: Oxyaquic Hapludults (PAa-Argissolo Amarelo Alumínico plintossólico)										
A1	10YR 3/3	we	sm & md	ang.bl & sg	sof	v.fri to lo	n.plas & n.sti	pla	grad	
A2	10YR 3/4	we	md & sm	ang.bl	s.hd to hd	fri	n.plas & n.sti	pla	cl	
AB	10YR 4/4	we	md & lar	ang.bl	hd	fri	s.plas to plas & sti	pla	grad	
BA	10YR 4/6	we to mod	md	sub & ang.bl	hd	fri	v.plas & sti to v.sti	pla	cl	
Btf1	7.5YR 5/8 e 10YR 5/3	mod mod	lar md	prism ang & sub.bl	hd	fri to fir	plas & v.sti	wav	grad	
Btf2	10YR 6/1 e 10 R 3/6	str str	lar lar & md	prism ang.bl	e.hd	fir	n.plas to s.plas & s.sti to sti	wav	grad	
Btf3	10YR 5/1 and 7.5YR 6/8	str str	lar lar	prism ang.bl	e.hd	v.fir to e.fir	n.plas to s.plas & s.sti	-	-	
P1T2: Arenic Hapludults (PBACva-Argissolo Bruno-Acinzentado Ta Alumínico abruptico arênico)										
A1	10YR 3/3	we	sm	sub.bl & sg	lo	v.fri	n.plas & n.sti	pla	grad	
A2	10YR 3/2	we	md	sub.bl & sg	sof	v.fri	n.plas & n.sti	pla	cl	
A3	10YR 3/2.5	we	lar & md	sub.bl	sof	fri	n.plas & s.sti	pla	cl	
BAt	10YR 3/3	we & mod we to mod	md md & sm	prism ang & sub.bl	hd	fri to fir	v.plas & sti	pla	grad	
Bt	10YR 3/4 and 2.5YR 3.5/6	mod mod	lar lar & md	prism sub.bl	v.hd	fir	s.plas & s.sti	pla	grad	
BC	5YR 4/6 and 7.5YR 5/1				hd	fri to fir	s.plas to plas & sti	pla	cl	
P2T2: Mollic Hapludalfs (TCK-Luvissole Crômico Carbonático solódico)										
A	10YR 3.5/2.5	we	md & lar	sub.bl	sof	fri	plas & s.sti to sti	pla	abrp	
Btxn	10YR 5/4	mod mod to str	lar & md lar	ang.bl sub.bl	e.hd	e.fir	v.plas & sti	pla	cl	
Btkn	5YR 5/7	we to mod	md	ang.bl	e.hd	v.fir	s.plas & sti	pla	grad	

Continue

Continuation

P3T2: Plintic Paleudults (FTd- <i>Plintossolo Argilúvico Distrófico abruptico</i>)									
A1	7.5YR 4/4	we	sm	gran & sg	sof	lo & v.fri	n.plas & s.sti	pla	grad
A2	10YR 4/4	we	md	sub & ang. bl e sg	s.hd to hd	fri	n.plas & s.sti	pla	abrp
2Btf1	5YR 4/5 e 2.5YR 4/6	we to mod	md	sub.bl	s.hd	fri to fir	s.plas & s.sti to sti	pla	grad
2Btf2	10R 4/8 and 5YR 4/6	mod mod	lar md & sm	prism ang.bl	e.hd	fir	n.plas to s.plas & sti	pla	grad
2Btf3	7.5YR 5/7 and 10R 4/8	mod mod	lar md	prism ang & sub.bl	v.hd	fir	plas & sti	-	-
P1T4: Oxyaquic Hapludalfs (TXp- <i>Luvissolo Háplico Pálico endorredóxico</i>)									
A1	10YR 3/2	we	sm	gran & sg	sof	lo & v.fri	n.plas & s.sti	pla	grad
A2	10YR 4/3.5	we	lar & md	ang.bl	s.hd	fri	n.plas & s.sti to sti	pla	cl
AB	10YR 3/4	we	lar & md	ang.bl	s.hd to hd	fri to firm	plas & sti	pla	abrp
BAt	10YR 2/2	mod	sm & md	ang & sub.bl	v.hd to e.hd	fri to firm	s.plas & s.sti	pla	grad
Bt	10YR 5/2 and 2.5YR 4/6	mod to str mod	lar & md md	ang.bl prism	e.hd	fir	s.plas to plas & s.sti	wav	cl
BC	7.5YR 4/3 and 2YR 3/6	we	lar & md	ang.bl	v.hd	fri to fir	s.plas & sti	pla	cl
P2T4: Arenic Kandiuudults (PVd- <i>Argissolo Vermelho Distrófico arênico</i>)									
A1	7.5YR 3/3	we	md & sm	gran & sg	sof	lo & v.fri	n.plas & n.sti	pla	grad
A2	5YR 3/4	we	md	sub.bl	sof to s.hd	v.fri	n.plas & n.sti	pla	cl
AB	5YR 4/6	we	md & sm	sub.bl	sof to s.hd	v.fri	n.plas & s.sti	pla	cl
BAt	5YR 3/3	we to mod	md	sub.bl	s.hd	fri	plas & sti	pla	cl
Bt1	2.5YR 3/6	mod	md & sm	sub.bl	hd	fir	plas & sti	pla	grad
Bt2	2.5YR 4/6	mod	md & sm	sub.bl	v.hd	fir	s.plas & s.sti	-	-

⁽¹⁾ we: weak; mod: moderate; str: strong. ⁽²⁾ v.sm: very small; sm: small; md: medium; lar: large. ⁽³⁾ gran: granular; sub.bl: subangular blocks; ang.bl: angular blocks; prism: prismatic; m: massive; sg: simple grain. ⁽⁴⁾ lo: loose; sof: soft; s.hd: slightly hard; hd: hard; v.hd: very hard; e.hd: extremely hard. ⁽⁵⁾ lo: loose; v.fri: very friable; fri: friable; fir: firm; v.fir: very firm; e.fir: extremely firm. ⁽⁶⁾ n.plas: non-plastic; s.plas: slightly plastic; plas: plastic; v.plas: very plastic; n.sti: non-sticky; s.sti: slightly sticky; sti: sticky; v.sti: very sticky. ⁽⁷⁾ pla: plan; wav: wavy. ⁽⁸⁾ cl: clear; grad: gradual; abrp: abrupt; dif: diffuse.

and centimeter dimensions, occur from the top of the B horizon and increase in depth to the Bt3 horizon, and most of them are identified as plinthite in the field. Reddish plinthite nodules occur interspersed with grayish and whitish patches, indicative of iron-depleted areas during reduction episodes. Along the entire Bt horizon, some petroplinthite concretions were observed, also identified at the base of the profile in the eroded area.

Toposequence 4 (T4) profiles were sampled over the Pirambóia formation, in different topographic positions, but quite distant from each other. Imperfectly drained, P1T4 is located at a lower elevation (146 m) than the well-drained P2T4 (165 m), previously described. The P1T4 has slope around 4 %, in a gently undulating relief area with low topographic gradient, being developed on siltstones. It has high amounts of reddish mottles, similar to plinthite, surrounded by grayish patches of iron depletion, whose amounts increase in the Bt to BC horizons. In C/Cr, a more grayish matrix predominates, which appears to result from the alteration of the red rock by reduction process.

The P1T1 presents a sandy texture from the soil surface to a depth greater than 1.00 m, with a very high textural ratio (TR = 4.8; calculated from average clay content in B horizon by average clay content in A horizon), denoting a strong increase in clay

Table 2. Chemical and physical data of soil profiles studied

Horizons	Layer m	Granulometric composition			pH(H ₂ O) ⁽¹⁾	Org. C g kg ⁻¹	S g kg ⁻¹	Al ³⁺ cmol _c kg ⁻¹	T cmol _c kg ⁻¹	V %
		Sand	Silt	Clay						
P1T1: Arenic Kanhapludults (PVd-Argissolo Vermelho Distrófico espessarênico abruptico)										
A1	0.00-0.23	852	68	80	5.53	4.2	1.42	0.16	2.63	54
A2	0.23-0.70	834	86	80	4.67	1.7	0.85	0.58	2.38	36
AE	0.70-0.90/0.95	857	73	70	4.88	1.6	0.42	0.60	1.34	31
E	0.90/0.95-1.10	837	113	50	5.07	0.9	0.26	0.46	0.87	30
Bt1	1.10-1.20	643	87	270	4.71	3.9	1.01	1.95	4.04	25
Bt2	1.2-1.77	500	70	430	4.95	3.7	2.83	2.32	6.35	45
Bt3	1.77-2.44	611	79	310	5.11	1.9	2.26	2.24	4.94	46
BC	2.44-2.88	743	47	210	4.93	2.3	1.28	1.72	3.38	38
P2T1: Oxyaquic Hapludults (PBACva-Argissolo Bruno-Acinzentado Ta Alumínico abruptico endorredóxico)										
A1	0.00-0.20	797	83	120	4.76	7.8	1.33	1.70	4.37	30
A2	0.20-0.42	762	78	160	4.86	7.2	1.31	2.61	5.36	24
2BA	0.42-0.63	474	136	390	4.96	10.0	4.27	8.63	13.46	32
2Bt	0.63-1.25/1.40	598	132	270	5.25	3.9	6.55	9.62	15.47	42
2BC	1.25/1.40-1.70/1.80	713	67	220	5.44	1.6	10.04	5.71	14.75	68
P3T1: Oxyaquic Hapludults (PAa-Argissolo Amarelo Alumínico plintossólico)										
A1	0.00-0.28	801	89	110	4.96	6.6	1.42	0.66	2.91	49
A2	0.28-0.50	609	261	130	4.89	4.5	0.61	1.62	3.06	20
AB	0.50-0.66	680	120	200	4.88	4.3	0.84	2.46	3.90	21
BA	0.66-0.82	602	148	250	5.01	5.6	1.30	3.29	5.56	23
Btf1	0.82-1.15/1.25	477	163	360	5.04	4.7	1.94	5.55	7.92	25
Btf2	1.15/1.25-1.7/1.85	505	175	320	5.29	2.6	3.14	4.56	8.00	39
P1T2: Arenic Hapludults (PBACva-Argissolo Bruno-Acinzentado Ta Alumínico abruptico arênico)										
A1	0.00-0.18	845	75	80	4.83	6.4	1.72	0.59	3.32	52
A2	0.18-0.34	833	77	90	4.61	5.9	1.28	1.22	4.03	32
A3	0.34-0.51	764	96	140	4.69	5.7	1.50	1.80	4.77	31
BAt	0.51-0.65	597	93	310	4.87	9.2	2.24	4.98	8.90	25
Bt	0.65-0.96	565	65	370	5.06	7.1	1.80	6.10	8.86	20
BC	0.96-1.15	681	59	260	5.02	4.2	1.43	6.28	7.19	20
P2T2: Mollic Hapludalfs (TCK-Luvissole Crômico Carbonático solódico)										
A	0.00-0.35	620	256	124	5.97	10.6	8.26	0.34	10.34	80
Btxn	0.35-0.58	478	308	214	6.43	5.1	10.16	1.25	12.41	82
Btkn	0.58-0.80	162	564	274	8.81	1.9	24.94	0.00	24.94	100
P3T2: Plintic Paleudults (FTd-Plintossolo Argilúvico Distrófico abruptico)										
A1	0.00-0.22	728	182	90	4.93	5.0	1.30	0.74	2.84	46
A2	0.22-0.60	728	182	90	4.68	3.3	0.99	0.79	2.35	42
2Btf1	0.60-0.78	502	168	330	4.94	4.9	2.26	2.77	6.34	36
2Btf2	0.78-1.20	510	140	350	4.95	4.0	2.62	3.02	6.57	40
2Btf3	1.20-2.00 ⁺	500	150	350	5.17	2.3	3.34	2.46	6.20	54
P1T4: Oxyaquic Hapludalfs (TXp-Luvissole Háptico Pálico endorredóxico)										
A1	0.00-0.11	749	121	130	5.35	12.8	4.50	0.07	6.21	72
A2	0.11-0.38	733	143	124	5.27	6.4	3.49	0.35	5.02	70
AB	0.38-0.48	607	119	274	4.97	7.7	5.24	2.99	10.06	52

Continue

Continuation

BAt	0.48-0.70	374	172	454	5.26	10.6	9.98	7.29	18.89	53
Bt	0.70-0.85/0.98	345	241	414	5.60	5.7	21.06	8.00	29.21	72
BC	0.85/0.98-1.25	580	196	224	5.78	3.5	19.98	3.72	23.51	85
P2T4: Arenic Kandiuults (PvD-Argissolo Vermelho Distrófico arênico)										
A1	0.00-0.20	823	63	114	5.01	6.5	1.30	0.61	2.94	44
A2	0.20-0.55	812	74	114	5.14	3.8	1.21	0.64	2.68	45
AB	0.55-0.67	737	89	174	5.10	4.9	2.01	0.91	4.11	49
BAt	0.67-0.77	584	82	334	5.06	8.2	3.21	1.62	6.42	50
Bt1	0.77-0.98	454	102	444	5.00	7.3	3.51	2.23	7.37	48
Bt2	0.98-1.75 ⁺	481	125	394	4.96	4.4	2.64	2.85	6.00	44

⁽¹⁾ At a soil:solution ratio of 1:1.

from horizon A to B. In addition, the soil showed abrupt textural change (ATC), with low activity clay in Bt. Clay skins are present in a scarce and weak degree in Bt1, and abundant and strong in Bt2 and Bt3, represented by depositions similar to clay-humus and, or iron-clay coatings. The subsurface horizon showed base saturation below 50 % (dystrophic character), Al^{3+} contents around $2 \text{ cmol}_c \text{ kg}^{-1}$ and aluminum saturation (m%) greater than 50 % in most sub-horizons.

Texture is sandy clay in 2BA and sandy clay loam in 2Bt and 2BC in the P2T1 profile, with high activity clay (Ta) in all sub-horizons, but with low base saturation in most of B. The TR was of 2.1, with an increase of clay for the identification of the argillic horizon, in addition to the occurrence of ATC. In the field, however, clay skins were not identified. The predominant color was dark brown at the top of B and brown at 2Bt and 2BC. The B sub-horizons have high Mg^{2+} and Ca^{2+} contents, but Al^{3+} are even higher, surpassing the sum of cations.

In P3T1, the subsurface horizon showed a TR of 2.2; however, the clay content in the transition from AB to BA was not significant enough to characterize ATC. It presented low activity clay (Tb) and very high contents of exchangeable aluminum, which exceed the sum of bases. No clay skins was observed. The dominant color/hue was 7.5YR or yellower in most of the first 1.00 m of the B horizon. There is an intense amount of reddish, prominent and distinct mottles and/or plinthite in horizons Bt_{f2} and Bt_{f3}, interspersed with gray spots, characterizing plinthic features in this soil.

The P1T2 soil presented a sandy texture from the surface to a minimum of 0.50 m in depth, with a high textural ratio (TR = 3.2) and a considerable increase in the clay content from A3 to BAt, indicating an ATC. The subsurface horizon showed high activity clay (Ta) in BAt and BC, and low activity clay (Tb) in Bt, but showed low base saturation in all sub-horizons. There was also an acid reaction phase with high amounts of exchangeable Al and Al saturation higher than 50 % with low levels of Ca^{2+} and Mg^{2+} . No clay skins were identified in B sub-horizons.

In the P2T2, the Btx sub-horizon showed a slightly acidic reaction phase, while in the underlying horizons, the pH value was very high (alkaline). The average clay content in B is 244 g kg^{-1} , and TR was 1.9, denoting a high increase in clay content. In this profile, however, there was no ATC, and also no clay skins evidence. Horizon B showed high activity clay (Ta) and high base saturation (eutrophic). The expressive presence of calcium carbonate concretions spread over the Btk and Cr horizons, together with the strong bubbling observed in the field tests with 20 % HCl, indicates a carbonate feature. Its chemical properties, different from other soils, are related to the profile being developed from pelitic substrate with limestone cementation in the Sanga do Cabral

formation. The soil also has chromatic colors in B horizons, very hard consistency and high sodium levels in the Btxn.

The P3T2 is moderately drained, with a TR of 3.8, indicating an expressive textural gradient, and has plinthite-like materials in all B sub-horizons. In the transition between the horizons, the amount of clay increased from 90 g kg⁻¹ in A2 to 330 g kg⁻¹ (more than three times higher) in Btf1. No clay skins were detected. The subsurface horizon showed low activity clay (Tb), with base saturation below 50 % (dystrophic), except in 2Btf₃. Despite the low pH, the exchangeable aluminum content is relatively low in this soil. The plinthite-like materials occur throughout Btf₂ and Btf₃ in the form of red aggregates, subscribed by the f symbol, interspersed with grayish and whitish spots.

Texture of the subsurface P1T4 B horizons is clay in BA_t and B_t, and sandy clay loam in BC, with very high activity clay (Ta) in all of these sub-horizons. The TR was 2, without ATC. There was also no clay skins. The predominant color at the top of the B (BA_t) was very dark brown and grayish brown in B_t, with an intense presence of mottles and iron depletion spots in horizons B_t and BC. The profile showed a eutrophic character (high base saturation) with elevated amounts of calcium and magnesium, but simultaneously high levels of “exchangeable” Al (7.29 to 8 cmol_c kg⁻¹ in BA_t and B_t, respectively). A plinthic-like material was noticed, in addition to strong redoximorphic features.

The A horizon of the P2T4 showed a sandy texture in the first 0.50 m, with a significant increase in clay, characterized by the high textural gradient. Despite this, the soil did not present ATC. The soil texture in the B_{t1} and B_{t2} horizons is clay to sandy clay, and sandy clay loam in the BA_t, with low activity clay. Clay skins were present in abundant and moderate degrees in B_{t1}, and common and moderate degrees in B_{t2}. The dominant hue in B was 2.5YR, with dark red and red colors. Horizon B showed a pH(H₂O) close to 5, exchangeable Al content lower than 4 cmol_c kg⁻¹ and base saturation below 50 % (dystrophic) but with a small increase in the base content (S) according to depth.

The results with iron and aluminum concentrations from different extraction solutions, and molecular relationships can be found in table 3. In the case of iron, all horizons from different soils presented the following content behavior: Fe_s > Fe_d > Fe_o. The Fe₂O₃ content varied between 4.06 g kg⁻¹ in P1T2 to 15.63 g kg⁻¹ in P2T2 for horizon A; and between 19.13 g kg⁻¹ in P2T2 to 38.31 g kg⁻¹ in P1T1 for horizon B. On surface (horizon A) the P1T2 profile had the lowest DCB iron content (2.99 g kg⁻¹ of Fe₂O₃), while in the P1T1 profile the highest values (6.47 g kg⁻¹ of Fe₂O₃). The Fe_d variation between the profiles follows the sequence below: P1T1 > P2T1 > P2T2 > P2T4 > P3T1 > P3T2 > P1T4 > P1T2. In the subsurface (horizon B), profile P2T2 had the lowest iron DCB values (5.62 g kg⁻¹ of Fe₂O₃), with profile P1T1 presenting the highest value (33.45 g kg⁻¹ de Fe₂O₃), considering the following order: P1T1 > P2T4 > P3T1 > P3T2 > P1T2 > P2T1 > P1T4 > P2T2.

The surface diagnostic horizons presented an Fe_o variation between 0.59 to 2.6 g kg⁻¹ of Fe₂O₃. The values presented the following sequential order: P2T2 > P1T4 > P2T1 > P1T2 > P3T1, which indicates additional iron contribution in primary minerals or more ferric smectites present in these soils; and P2T4 > P1T1 > P3T2, roughly accompanying a reduction in its contents with the improvement in surface drainage conditions.

In the subsurface B horizon, the Fe_o content was as follows: P2T4 > P1T2 > P1T1 > P3T2 > P1T4 > P2T1 > P3T1 > P2T2, with values ranging from 0.36 to 3.43 g kg⁻¹ of Fe₂O₃. The higher Fe_o contents coincided with the soils located in the highest positions of the toposequence, which probably have higher iron contents in their substrates.

In most profiles, both in horizon A and in B, the Fe_d/Fe_s ratio was greater than 0.5, showing the dominance of iron in the form of oxides, except for the P2T2 and P1T4 profiles, which seems to indicate additional iron contribution in primary minerals or more ferric smectites present in these soils.

Table 3. Iron and aluminum contents of the air-dried fine earth extracted from sulfuric acid, ammonium acid oxalate and sodium dithionite-citrate-bicarbonate and molecular relationships of the soil profiles under study

Horizons	Al ₂ O ₃ ⁽¹⁾	Fe ₂ O ₃ ⁽¹⁾	Al ₂ O ₃ ⁽²⁾	Fe ₂ O ₃ ⁽²⁾	Fe ₂ O ₃ ⁽³⁾	Molecular relationships						
						Ki ⁽⁴⁾	Kr ⁽⁴⁾	Fe _o /Fe _d	Al _s /Fe _s	Al _o /Fe _o	Fe _o /Fe _s	Fe _d /Fe _s
————— g kg ⁻¹ —————												
P1T1: Arenic Kanhapludults (PVd-Argissolo Vermelho Distrófico espessarênico abruptico)												
A2	8.77	7.96	1.21	0.69	6.47	2.8	2.2	0.11	0.83	1.32	0.09	0.81
Bt2	99.67	38.31	3.08	2.23	33.45	2.2	1.7	0.07	1.97	1.04	0.06	0.87
Cr	-	-	1.10	0.70	6.30	3.4	2.6	0.11	-	1.23	-	-
Bt2 (clay skins)	-	-	5.45	4.37	37.03	-	-	0.12	-	0.94	-	-
P2T1: Oxyaquic Hapludults (PBACva-Argissolo Bruno-Acinzentado Ta Alumínico abruptico endorredóxico)												
A2	17.00	9.02	2.72	1.97	6.43	3.4	2.7	0.31	1.43	1.04	0.22	0.71
2Bt	68.42	21.00	4.59	1.46	13.19	3.0	2.5	0.11	2.47	2.37	0.07	0.63
2C	33.51	11.59	1.29	0.41	5.70	3.3	2.8	0.07	2.19	2.39	0.04	0.49
R	31.23	10.73	1.19	0.19	6.33	2.3	1.8	0.03	2.20	4.97	0.02	0.59
2BC (Red S.)	-	-	3.15	4.09	18.38	-	-	0.22	-	0.58	-	-
2BC (Gr. S.)	-	-	3.62	0.66	1.60	-	-	0.41	-	4.13	-	-
P3T1: Oxyaquic Hapludults (PAa-Argissolo Amarelo Alumínico plintossólico)												
A2	24.45	4.10	1.54	0.95	5.33	3.3	2.6	0.18	4.52	1.23	0.23	1.30
Bt2f	61.12	30.56	2.98	1.25	19.62	2.7	2.2	0.06	1.51	1.80	0.04	0.64
R	27.67	17.73	0.79	0.27	14.00	2.5	1.9	0.02	1.18	2.29	0.01	0.79
Bt3f (Red S.)	-	-	3.59	3.96	43.37	-	-	0.09	-	0.68	-	-
Bt3f (Gr. S.)	-	-	3.16	0.70	5.44	-	-	0.13	-	3.44	-	-
P1T2: Arenic Hapludults (PBACva-Argissolo Bruno-Acinzentado Ta Alumínico abruptico arênico)												
A2	12.83	4.06	1.27	0.99	2.99	4.8	3.8	0.33	2.39	0.97	0.24	0.74
Bt	69.84	21.75	3.89	3.23	13.41	2.7	2.2	0.24	2.43	0.91	0.15	0.62
C/Cr	40.34	10.33	2.34	1.85	6.43	2.9	2.3	0.29	2.96	0.96	0.18	0.62
R	-	-	-	-	-	3.2	2.8	-	-	-	-	-
P2T2: Mollic Hapludalfs (TCK-Luvissole Crômico Carbonático solódico)												
A	38.07	15.63	2.43	2.60	6.31	3.3	2.6	0.41	1.84	0.71	0.17	0.40
Bt	55.27	19.13	1.31	0.36	5.62	3.8	3.1	0.06	2.19	2.82	0.02	0.29
Cr	53.58	24.19	0.87	0.15	7.43	3.9	3.2	0.02	1.68	4.54	0.01	0.31
P3T2: Plintic Paleudults (FTd-Plintossolo Argilúvico Distrófico abruptico)												
A2	22.61	7.77	1.40	0.68	4.76	3.4	2.7	0.14	2.20	1.55	0.09	0.61
2Btf2	74.56	27.77	3.72	1.76	18.02	2.4	1.9	0.10	2.03	1.60	0.06	0.65
Cr	97.03	25.93	1.86	0.27	11.31	2.8	2.4	0.02	2.83	5.36	0.01	0.44
2Btf3 (Gr. S.)	-	-	2.76	0.91	6.11	-	-	0.15	-	2.31	-	-
2Btf3 (Red S.)	-	-	3.38	3.66	34.31	-	-	0.11	-	0.70	-	-
P1T4: Oxyaquic Hapludalfs (TXp-Luvissole Háplico Pálico endorredóxico)												
A2	25.21	9.20	1.48	2.05	3.68	4.8	3.7	0.56	2.07	0.55	0.22	0.40
Bt	92.36	37.83	4.45	1.47	12.84	4.2	3.1	0.11	1.85	2.29	0.04	0.34
C/Cr	60.15	26.33	1.17	0.82	9.87	3.8	2.9	0.08	1.73	1.09	0.03	0.37
R	-	-	-	-	-	3.9	3.0	-	-	-	-	-
P2T4: Arenic Kandiuults (PVd-Argissolo Vermelho Distrófico arênico)												
A2	30.91	9.15	0.77	0.81	6.28	3.1	2.4	0.13	2.56	0.72	0.09	0.69
Bt1	109.36	33.43	3.33	3.43	26.85	2.3	1.9	0.13	2.48	0.74	0.10	0.80
R	79.15	15.69	1.23	0.34	10.56	2.9	2.2	0.03	3.82	2.83	0.02	0.67

⁽¹⁾ Sulfuric Attack. ⁽²⁾ Oxalate. ⁽³⁾ DCB (sodium dithionite-citrate-bicarbonate). ⁽⁴⁾ XRF (X-ray fluorescence). Red. S.: redish spots; Gr. S.: greyish spots.

In the superficial horizon, the Fe_o/Fe_d ratio values varied from 0.11 in P1T1 to 0.56 in P1T4, while in the subsurface, the values ranged from 0.06 in the Bt_f₂ horizon of the P3T1 profile to 0.24 in the Bt of P1T2. The Al_o/Fe_s ratio was only less than 1 in the A2 horizon of the P1T1 profile. In the other soils, the aluminum values were exceptionally high compared to iron, with the ratio varying from 1.43 to 4.52 on the surface and 1.51 to 2.48 in horizon B.

The Al_o/Fe_o ratio showed high values that were higher than, or closer to 1, several times. The profiles/horizons that carried low crystallinity iron higher than the amorphous aluminum, provided by the Al_o/Fe_o being lower than 1, were A2 and Bt P1T2, A of P2T2, A2 of P1T4, and A2 and Bt1 of P2T4.

In all the samples evaluated, the levels of Fe₂O₃ in the segregations were higher than those found in the soil matrix and the rock, or in the underlying saprolite, with values of Fe₂O₃ oxalate in a range between 0.66 to 0.91 g kg⁻¹ in the matrix, and from 3.66 to 4.09 g kg⁻¹ in the segregations. The Fe₂O₃ DCB values ranged from 1.6 to 6.11 g kg⁻¹ in the matrix and 18.38 to 43.37 g kg⁻¹ in the segregations (Table 3).

The data for the profile's Ki and Kr indexes are shown in table 3, quantified by XRF in the clay fraction, Ki values were relatively high for the vast majority of soils, with values always greater than 2. Regarding Kr, all profiles had an index higher than 0.75, being in the most cases higher than 2.0.

The high textural gradient of the set of soils is presented in figure 4, where the distribution of the sand and clay fractions of each soil is shown according to the depth of the horizons and layers in the profiles (Tables 1 and 2).

The two red Ultisols (P1T1 and P2T4) did not show mottles and, or plinthite, and the mineralogy of the clay fraction was predominantly kaolinitic (Figure 5). In the P1T1, the kaolinite peak 001 was the most intense, being asymmetrical towards the lower 2θ angles, indicating a possible contribution of kaolinite with interstratification of layers 2:1, kaolinite-smectite (C-E) and kaolinite-vermiculite (C-V), as less likely (Figure 5a). Semi-quantitatively, the proportions of the clay minerals present in the sample of the Bt2 horizon of P1T1 are approximately 10 % of smectite layer 2:1 clay minerals and 90 % of kaolinite and C-E mixtures (Table 4).

In the Bt1 horizon of the P2T4, diffractograms show a predominance of kaolinite with good crystallinity (intense and symmetrical peaks at 0.72; 0.357 and 0.238 nm). It also has mica/illite (peaks around 1.007 and 0.498 nm), and a little vermiculite, with hydroxy-aluminium interlayer, or smectite with hydroxy-aluminum polymers between layers (Figure 5k).

In the yellow Ultisol (P3T1) the diffractogram (Figure 5d) indicates more intense peaks in the position of the kaolinite (0.717 nm), with the presence of interstratifications 1:1-2:1, possibly kaolinite-smectite. There is also a low intensity peak around 1.0 nm and a more intense peak at 1.447 nm, which respectively indicate micas (or illites) and 2:1 phyllosilicate with some interlayered Al polymers. Semi-quantitatively, the proportions of clay minerals present in the sample of the Bt_f₂ horizon are approximately 29 % smectites, 2 % micas (illites) and 69 % kaolinite (Table 4).

In the 2Bt_f₂ horizon of the P3T2 (plintic Paleudult) the diffractogram pattern (Figure 5h) was similar to that of the A2 horizon (data not shown), indicating the same mineralogical components, with more intense peak, but very asymmetrical, around 0.72 and 0.36 nm, possibly indicating kaolinite in association with kaolinite-smectite as dominant components. Type 2:1 phyllosilicate identified as smectite with hydroxy-aluminum polymers between layers occurs as a second component (peak at 1.55 nm). Illite (peaks at 1.0 and 0.5 nm) and quartz (peaks at 0.42 and 0.33 nm) were identified as the third and fourth components. Semi-quantification indicated approximately

10 % smectite with hydroxy-aluminum polymers between layers, 3 % illitic micas and 87 % kaolinite associated with kaolinite-smectite (Table 4).

Diffractiongram of the Btx horizon shows very sharp peaks at the position of 1.57 nm in the mollic Hapludalf of the Sanga-do-Cabral formation (P2T2). It also shows the main quartz at 0.33 nm, and the illite peak at 0.99 nm in Mg+EG and 1.00 nm in Mg (Figure 5g). Quantitatively, the proportions of clay minerals present in the sample of the Btx horizon are approximately 99 % of smectites along with interstratified chlorite-smectite and only

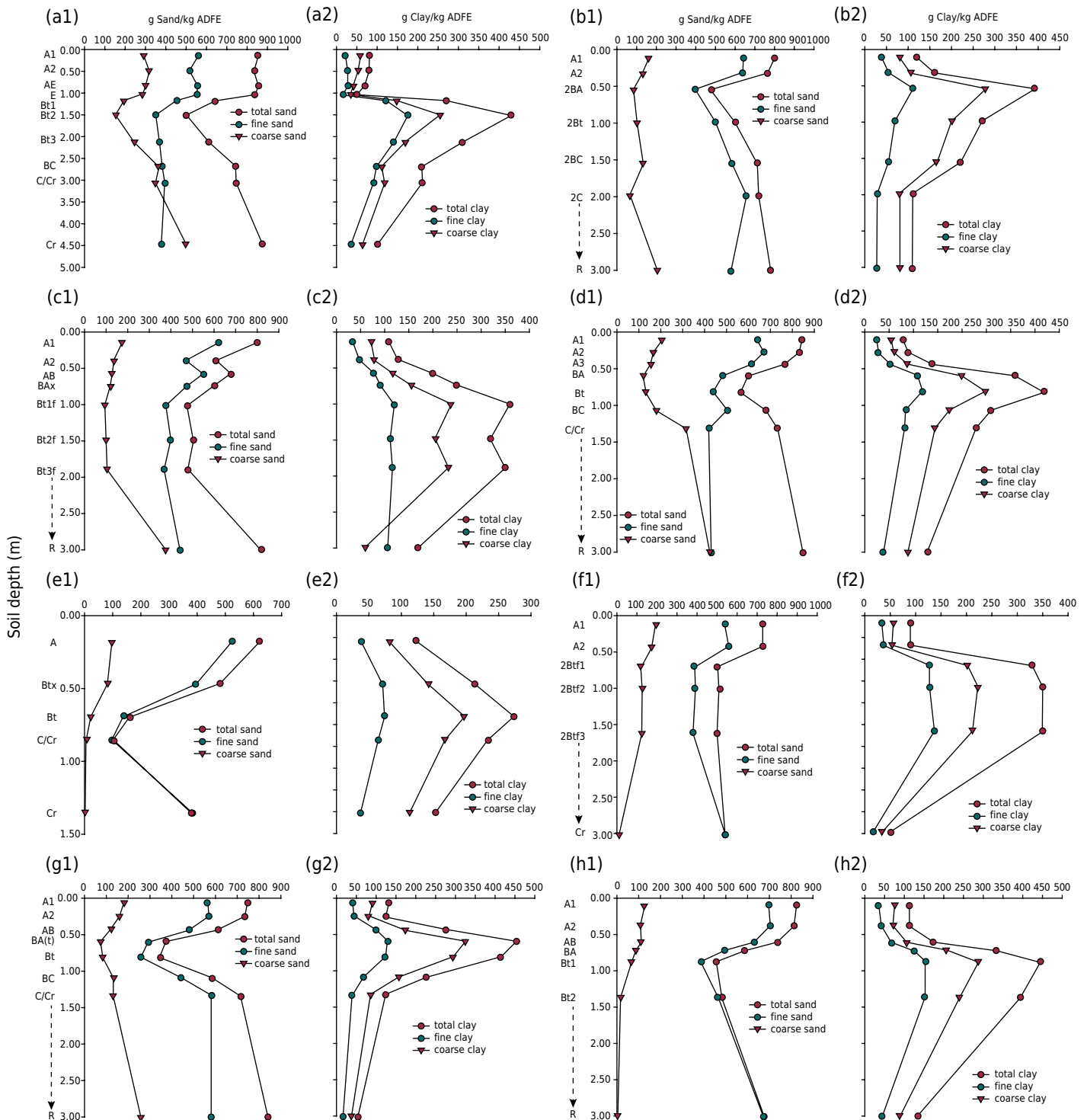


Figure 4. Distribution of soil granulometric fractions according to the depth of horizons and layers in the studied soil profiles: (a1 and a2) P1T1; (b1 and b2) P2T1; (c1 and c2) P3T1; (d1 and d2) P1T2; (e1 and e2) P2T2; (f1 and f2) P3T2; (g1 and g2) P1T4; (h1 and h2) P2T4.

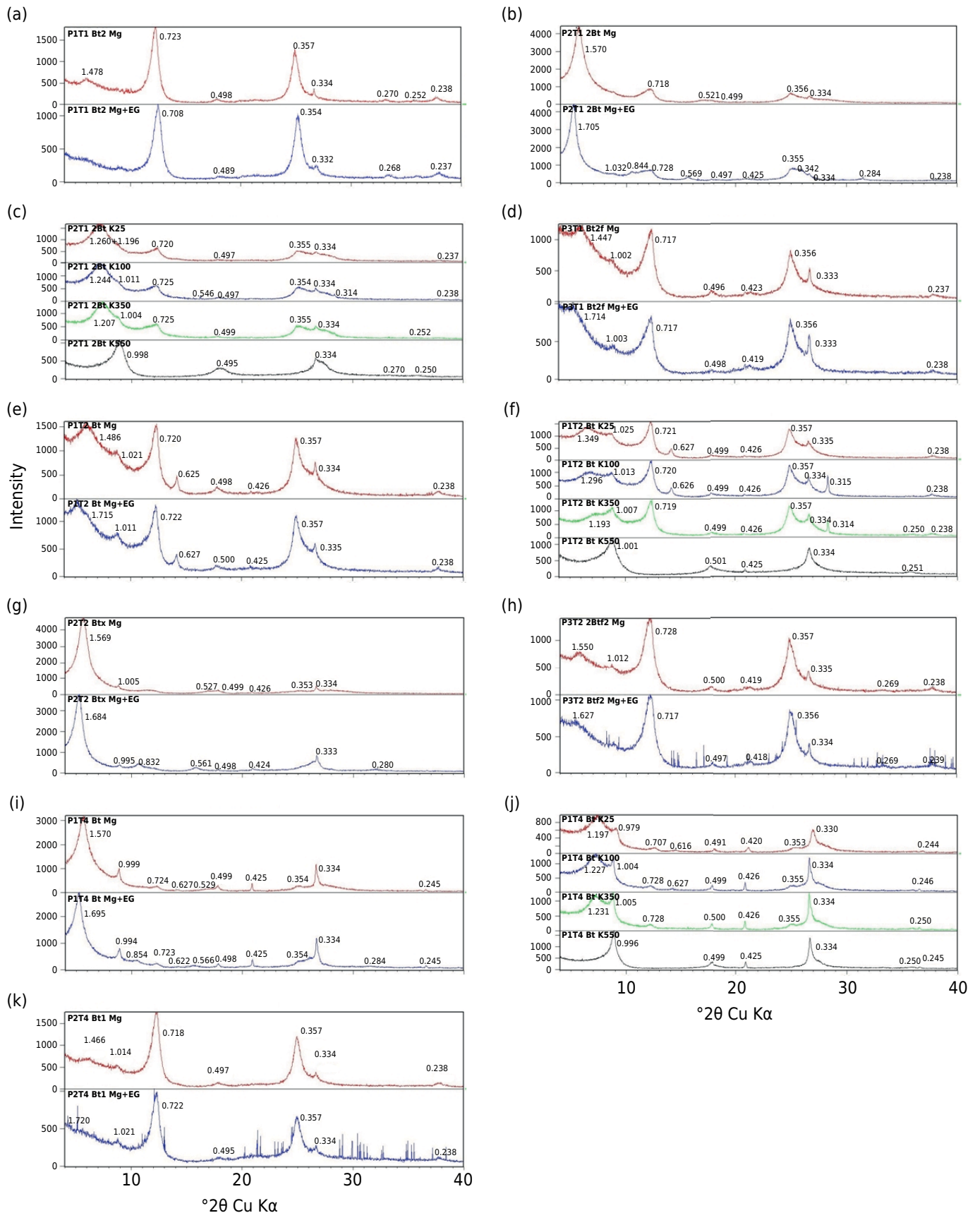


Figure 5. X-ray diffractograms of the clay fraction of horizons B of the studied soil profiles. Samples subjected to saturation treatment with magnesium (Mg) and magnesium saturated with ethylene glycol vapor (Mg+EG): (a) P1T1-Bt2, (b) P2T1-2Bt, (d) P3T1-Btf2, (e) P1T2-Bt, (g) P2T2-Btx, (h) P3T2-2Btf2, (i) P1T4-Bt and (k) P2T4-Bt1. Samples subjected to potassium saturation treatment at different heating levels, room temperature (K25), at 100 °C (K100), 350 °C (K350) and 550 °C (K550): (c) P2T1-2Bt, (f) P1T2-Bt and (j) P1T4-Bt. Nanometer values.

Table 4. Semiquantitative data of clay minerals by XRD technique

Horizon	Relative proportion of clay minerals ⁽¹⁾		
	2:1HE	Mi/Il	Ct/C-E
P1T1: Arenic Kanhapludults (PVd-Argissolo Vermelho Distrófico espessarênico abruptico)			
A2	10.40	2.00	87.60
Bt2	9.60	-	90.40
Cr	-	1.22	98.78
P2T1: Oxyaquic Hapludults (PBACva-Argissolo Bruno-Acinzentado Ta Alumínico abruptico endorredóxico)			
A2	57.18	4.65	38.17
2Bt	84.75	-	15.25
R	88.80	1.82	9.38
P3T1: Oxyaquic Hapludults (PAa-Argissolo Amarelo Alumínico plíntossólico)			
A2	17.55	9.15	73.30
Btf2	28.78	2.36	68.86
R	24.04	1.78	74.18
P1T2: Arenic Hapludults (PBACva-Argissolo Bruno-Acinzentado Ta Alumínico abruptico arênico)			
A2	44.37	11.42	44.21
Bt	37.54	6.88	55.58
R	74.20	1.20	24.60
P2T2: Mollic Hapludalfs (TCK-Luvissolo Crômico Carbonático solódico)			
A	93.12	-	6.88
Btx	99.67	0.33	-
Cr	99.50	-	-
P3T2: Plintic Paleudults (FTd-Plintossolo Argilúvico Distrófico abruptico)			
A2	20.23	7.50	72.27
2Btf2	9.80	2.60	87.60
Cr	14.27	8.30	77.43
P1T4: Oxyaquic Hapludalfs (TXp-Luvissolo Háplico Pálico endorredóxico)			
A2	79.92	13.44	6.64
Bt	93.87	4.46	1.67
R	96.72	1.44	1.84
P2T4: Arenic Kandiodults (PVd-Argissolo Vermelho Distrófico arênico)			
A2	4.10	6.50	89.40
Bt1	5.40	2.10	92.50
R	63.10	2.24	34.66

⁽¹⁾ Percentage obtained from the relation between the areas of the peaks of the clay minerals considered: 2:1HE: 2:1 (smectite or vermiculite) and/or interstratified 2:1 and/or EHE and/or VHE; Mi/Il: mica (illite); Ct/C-E: kaolinite and/or interstratified kaolinite.

1 % of illitic micas (Table 4). Interstratified cholate-smectite is indicated by the permanence of a peak around 1.23 in the treatment with K and heating to 350 °C.

There was no plinthite and expressive mottling in this soil due to its sloping position and better drainage. The pattern of the diffractograms is very similar in the samples saturated with Mg and K in Bt horizons of P2T1 and P1T2 Hapludults, and in P1T4 Hapludalfs, indicating practically the same clay minerals (Figures 5b, 5c, 5e, 5f, 5i and 5j). Symmetrical, intense and sharp peaks with Mg (1.570 nm) indicate a predominance of smectites over kaolinite. In samples saturated with K and heated, gradual contraction of the layers is observed, but even after heating to 350 °C, a complete collapse is not observed, which suggests the presence of interlayered material preventing the

contraction. The collapse only occurs at 550 °C, at spacing values of 1.003 nm, but even so, with asymmetry for lower 2θ angles. As expected, heating to 550 °C destroys the kaolinites (Brindley and Brown, 1980), causing the peaks to disappear at 0.723 and 0.355 nm. In these soils, redoximorphic features are clearly observed due to the presence of intense mottling, forming areas of iron depletion represented by grayish spots interspersed with reddish nuclei, showing the processes of oxyreduction from the top of the B horizon to the saprolite.

DISCUSSION

Selective extractions and molecular relationships

Levels of iron and aluminum oxides of the sulfuric attack showed great variation within the profile and between the different soils. However, the levels of Fe_2O_3 in all profiles were lower than 80 g kg^{-1} , characterizing hypoferric soils (Santos et al., 2018). These low values in the soil are because the source material is composed of sedimentary rocks with a low concentration of iron in their constitution. The results would include both Fe from oxides and Fe and part of Al from silicate minerals (Espírito Santo, 1988). An increase in the levels of Fe_s and Al_s can be seen in all profiles from the surface horizons towards the subsurface horizons. This behavior is typical of soils with high textural contrast due to the increase in clay content and reduction of silt and/or sand in relation to surface horizons. After reaching a maximum value in some part of the B horizon, they tend to decrease towards the rock or saprolite, with the exception of the P2T2 where there was a small increase in the content of Fe_s , and in the P3T2, where there was an increase in Al_s .

Levels of Fe_d increased in depth in practically all profiles, with the exception of P2T2, which presented a value in the Bt horizon lower than A. Higher levels of iron oxides (Fe_d) were observed in the subsurface diagnostic horizons (B textural) coinciding with the horizons of greater clay accumulation, such as Fe_s . Sodium dithionite-citrate-bicarbonate (DCB) is used when determining the Fe extracted successively by the selective dissolution of pedogenetic iron oxides, which includes both crystalline (hematite and goethite) and low crystallinity forms (Mehra and Jackson, 1960; Holmgren, 1967; Inda Jr and Kämpf, 2003). Its increase in depth generally accompanies the increase in clay content (Kämpf and Curi, 2000). The distinct levels of Fe_d between the profiles may be due to differences not only in the constitution of the source material, but also in the drainage conditions of the profiles affected by the relief and the intrinsic properties of each soil. This interpretation is supported by data from the two red Ultisols profiles of the Pirambóia formation (P1T1 and P2T4), which present a markedly and well-drained class, respectively, and with slightly higher Fe_d values in relation to the other profiles.

Pattern of the variation of Fe_o contents was different in relation to Fe_d . In profiles P2T1, P2T2 and P1T4, the Fe_o content decreased from horizon A to B, while in the other profiles there was an increase. The low values of the Fe_o/Fe_d ratio indicate that iron oxides are predominantly crystalline in both horizons (A and B) of all profiles. The Fe_o/Fe_d ratio decreases in depth in practically all soils, with the exception of the P2T4, in which it remains constant. This general pattern shows that the most crystalline pedogenetic oxides (Fe_d) are found mostly in the subsurface horizons. Higher levels of organic C in the surface horizons may partly explain the higher Fe_o/Fe_d ratio considering that organic matter can inhibit Fe crystallization (Schwertmann, 1964; Schwertmann and Taylor, 1989).

The Al_s/Fe_s ratio in the soil is used to proportionally compare the total levels of iron and aluminum extracted with strong acid, whose result reflects the nature of the source material (mineralogical composition) and the degree of pedogenesis, which, according to the data presented, indicate the chemical poverty in iron in the source materials.

The K_i and K_r indexes are used as a reference when studying the weathering rate in tropical and subtropical soils (Kehrig, 1949; Carvalho, 1956; Melo et al., 1995; Claessen, 1997). Considering the soils with the highest degree of evolution (red and plinthic Ultisols), the K_i values were between 2.2 and 2.7 in the B horizon, which is indicative of kaolinitic mineralogy with lesser participation of 2:1 phyllosilicates (Resende and Santana, 1988; IBGE, 2015), compatible with the observed mineralogical composition (Figure 5 and Table 4). Concerning the less evolved soils, constituted by the P2T1, P1T2, P2T2 and P1T4, the K_i values were even higher, with values consistent with the predominantly smectite mineralogy of these soils found using XRD, varying from 2.7 to 4.2 in the Bt horizons (Figure 5 and Table 4).

As the sedimentary rock is altered by weathering and as the degree of pedogenesis evolves, more intense Si losses occur in the subsurface horizons, and a relative increase in Fe, Al, culminating in very low K_r values, indicating an increase in the depth weathering rate (Santos, 2015). The fact that K_r values remains relatively high reveals that the degree of weathering varied from medium to high, with average values slightly below 2.0 in the Bt horizon of the red Ultisols, compatible with a more kaolinitic mineralogy, and higher than 2.0 in the other less evolved soils, where the participation of 2:1 clay minerals was high. In general, a trend towards the formation of 1:1 minerals (monosialitization) can be observed in profiles with a lower K_i ratio, because of the greater loss of silicon from the system due to better drainage conditions (Santos, 2015).

Argilluviation and ferrollysis

Occurrence of high textural contrast between horizons A or E, and Bt is a common feature in Ultisols and Alfisols in general, characterized by the increase of clay in depth and/or abrupt textural change, associated or not with clay skins (Santos et al., 2018). The origin of the textural gradient in soils can occur through the transport of clay in depth (clay illuviation), differences in the granulometric composition of the sedimentary strata of the source material, or due to lithological discontinuity caused by the deposition of layers of coarser sedimentary material on a pre-existing profile (Phillips, 2004; Michelon et al., 2010).

According to Soil Survey Staff (1999), the clay illuviation processes can be identified by increasing the ratio between fine clay and total clay, or between fine clay and coarse clay in depth. A generalized increase in the content of fine clay was observed in the textural B horizons of all profiles in relation to the overlying A horizons (Figure 4), but there was only a significant increase in A_f/A_c or A_f/A_r in the P1T1 profile, accompanied in the field by the presence of strong and abundant clay skins covering the structural aggregates. However, the argilluviation hypothesis cannot be ruled out in the other profiles, since the fine clay ratio data must be interpreted with caution, due to the instrumental limitations of the method used in its determination.

Furthermore, there are indications of the presence of lithological discontinuity in some profiles, as in P2T1, suggested by the presence of a gravel line between horizons A and Bt (Santos, 2015), which alerts to the fact that the clay illuviation process may not be the only one responsible for the formation of textural contrast (Michelon et al., 2010). Phillips (2004) points out that the textural contrast can also be originated by processes such as ferrollysis, selective erosion and clay neoformation. Ferrollysis is a soil formation process that causes disintegration of clays and/or inter-stratification of Al polymers in 2:1 clay minerals (Brinkman, 1970, 1977; Jimenez-Rueda and Demattê, 1988; Almeida et al., 1997; Oliveira Junior et al., 2017). It can be a complementary process responsible for forming strong textural contrast in soils due to an alternation sequence of repeated cycles of reduction and oxidation reactions by the temporary existence of a suspended water table (Schaefer et al., 2002).

An expressive part of the studied region's soils developed from the Pirambóia formation, especially those of the Oxyaquic Hapludults P2T1 and Oxyaquic Hapludalfs P1T4 classes, have temporary drainage restrictions and particular chemical properties, such as low pH (acid reaction) and high exchangeable aluminum content, generally associated with high levels of calcium and magnesium (Table 2). This atypical behavior seems to be related to the release of large amounts of Al resulting from the frequent alternation of oxy-reduction processes, which can promote the destruction of smectites, and/or the contribution of Al from hydrolysis of Al polymers between layers (Santos, 2015; Cunha et al., 2015).

Smectites are dominant in the underlying lithology of these profiles and are still quite preserved in the most superficial horizons (Figure 5). Our diffractograms (Figure 5) show expansion of the layers in treatments with ethylene glycol, but an only partial contraction of them in heating samples to 350 °C, indicating the presence of Al in the interlayer space. In these soils, the preservation of high amounts of smectites would therefore explain the higher base sum values associated with high exchangeable Al contents. In the other two soils with redoximorphic features (P3T1 and P1T2), although the diffractograms reveal a similar behavior for the smectites, they occur in smaller quantities (Table 4), which would explain the lower values of the sum of bases, but still maintaining high amounts of exchangeable Al.

This behavior suggests that a contemporary process of destruction of smectites must be taking place in all soils with redoximorphic features, releasing large amounts of aluminum in the current humid environment. This occurs due to the frequent alternation of reducing and oxidizing conditions in these soils indicated by morphological evidence such as the presence of red and yellow mottles, and areas with iron depletion. Aluminum probably forms amorphous polymers, which in large part are interlayered in the remaining smectite due to its positive charge. A similar interpretation is made by Cunha et al. (2015) with soil similar to that studied in the same region.

These results showed that the minerals of the smectite group are in destruction process by ferrolisis due to the current humid climate, resulting in the release of large amounts of Al (Table 2), while suggesting that this process is also implicated in the genesis of the high textural contrast of these soils.

Iron segregation and plinthization

Both directly in the field and later in a laboratory environment, the correct identification of segregations (nodules, concretions, mottles and plinthite) is not an easy task, due to a certain subjectivity in the criteria imposed on the pedologist in the assessment, raising doubts regarding the identification of these materials and the nature of the processes involved in its genesis.

In the Oxyaquic Hapludult P2T1, there was a concentration of Fe_2O_3 extracted by DCB and oxalate in the red spots of the 2BC horizon compared with the grayish residual matrix (iron depletion zone) and with the immediately overlying horizon (2Bt). The Fe_2O_3 content extracted by DCB and oxalate in the segregations was respectively 1.4 and 2.8 times greater than in the 2Bt horizon matrix, indicating that much of the iron accumulated in the segregations is still in less crystalline phases. The Fe_2O_3 content in the depletion zones was very low by the two extractors, indicating a marked iron loss. As the DCB mainly extracts crystalline iron oxides (Inda Jr and Kämpf, 2003), an increase of only 40 % in the segregations in relation to the matrix does not seem to constitute sufficient accumulation for the formation of plinthite, having been interpreted simply as mottle. This was confirmed later by the physical evaluations (Figure 6), where most segregations were not preserved after the various wetting and drying cycles. When comparing the contents of Fe_2O_3 DCB in the 2BC segregations (reddish spots) with that of the R layer, however, it is observed that they were about 3 times higher than

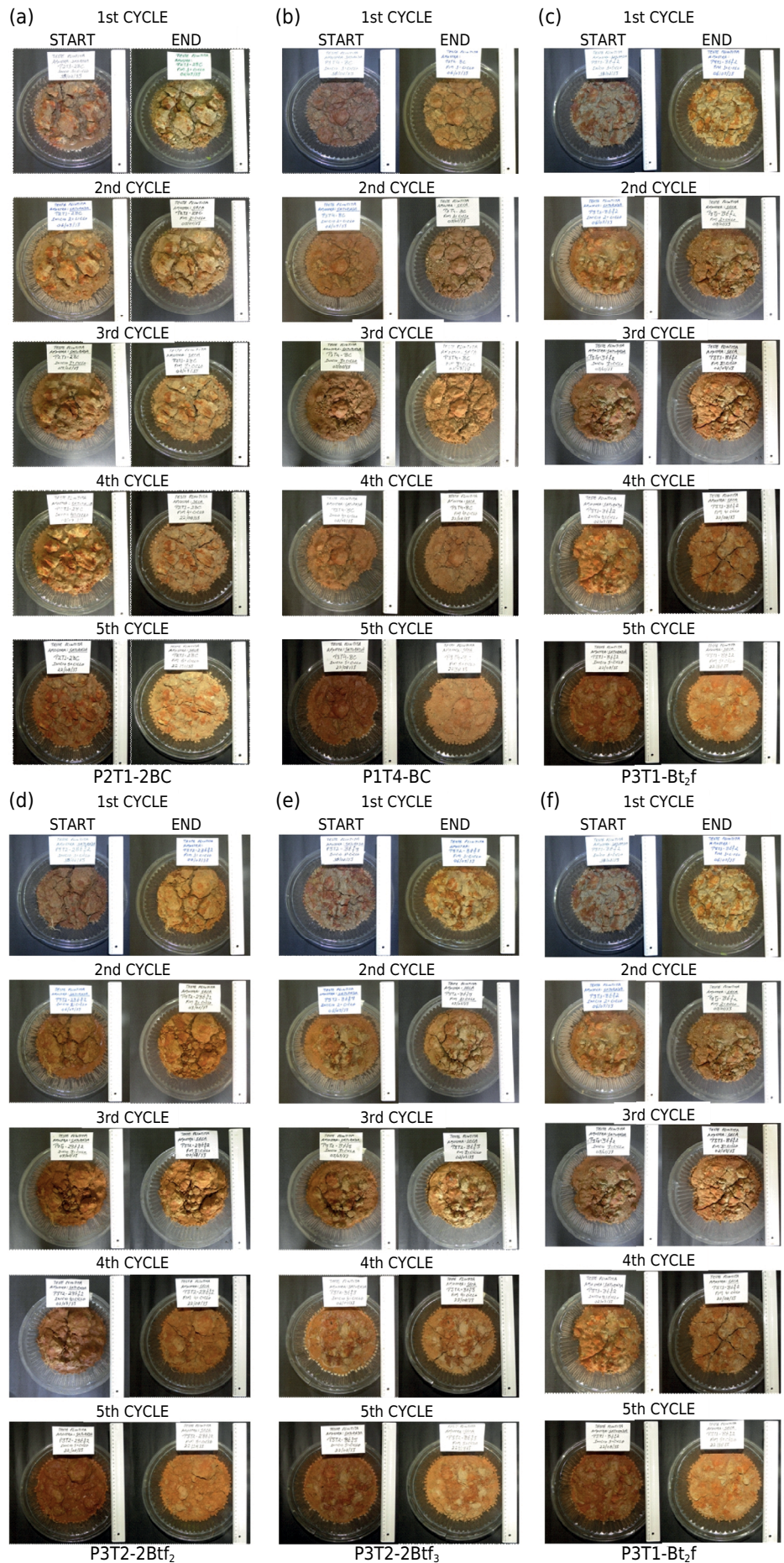


Figure 6. Plinthite visual test result from soil profile horizons submitted to repeated wetting and drying cycles. (a) 2BC-P2T1; (b) BC-P1T4; (c) Bt₂f-P3T1; (d) 2Bt₂, (e) 2Bt₃ of P3T2; and (f) Bt₂f-P3T1.

that, indicating that it is not actually remaining iron from alteration of the rock. The Fe_o/Fe_d ratio in the 2BC matrix was higher than in segregation, and this, in turn, was higher than in 2Bt (Table 3).

In the P3T1-PAa, a similar pattern is observed when compared to the previous profile, with Fe_2O_3 values (DCB and oxalate) in the segregation (red Btf₃ spots) respectively 2 and 3 times higher than the Btf₂ horizon, while the grayish matrix of Btf₃ presented much lower levels of Fe_2O_3 both in relation to segregation and in the matrix of the overlying horizon, but with a higher Fe_o/Fe_d ratio (Table 3). In relation to the rock, the Fe_2O_3 content in the Btf₂ matrix was only slightly higher, but it was about three times higher than the rock in the Btf₃ segregations. The Btf₂ (and Btf₃) horizon segregations in this soil were interpreted as plinthite because physical tests proved its presence in this horizon, but it was not proven in the horizon immediately above (Btf₁) (Figure 6).

The P3T2-FTd did not differ much from the previous profiles, with a concentration of Fe_2O_3 extracted by DCB and oxalate in the red segregations of 2Btf₃, in both cases, about two times higher than in the 2Btf₂ matrix. In the gray matrix, on the other hand, the Fe_2O_3 content by DCB was about six times less than in the segregations and three times less than in the 2Btf₂ horizon matrix. Likewise, the Fe_o/Fe_d ratio was higher in the 2Btf₃ matrix and with similar values between segregation and 2Btf₂ (Table 3). There was no exposure of fresh rock (R) in this profile, and only saprolite (Cr) was collected, whose content of Fe_2O_3 by DCB was about three times lower than in segregations. Although the results of the iron in the soil in question did not differ significantly from the other soils evaluated, after the five wetting and drying tests, the reddish segregations remained mostly aggregated, with little material disintegrated in smaller sets (Figure 6), having been interpreted as plinthite.

According to the criteria suggested for plinthite identification, the material from the 2BC horizons of P2T1 and BC belonging to P1T4 did not characterize its presence. When tested, they did not present a hard, or very hard consistency when dry, and firm consistency when wet. They had a brittle and friable appearance, disintegrating when pressed by the thumb and forefinger. When subjected to the wetting and drying cycles, the material collapsed, in addition to being fragmented, presenting a diameter of less than 2 mm mostly after the tests. Separating it from the soil matrix was also not possible.

In the P3T1, although the test did not reveal the presence of plinthite in Btf₁, it presented a plinthic horizon that coincided with Btf₂, with plinthite in sufficient quantity (volume $\geq 15\%$) and thickness (>0.15 m), but in a position that did not allow the requirement for *Plintossolos* in Brazilian Soil Classification System (SiBCS) (Santos et al., 2018). The P3T2, however, presented plinthite in sufficient volume and thickness to characterize the plinthic horizon (2Btf₂ and 2Btf₃) in the SiBCS, occurring in a diagnostic position for the order of *Plintossolos*.

It can be seen in the previous discussion that the amount of iron accumulated in the segregations alone, as well as the material's characteristic of being or not more or less easily separated from the rest of the soil matrix, do not guarantee the identification of the material as plinthite. Many segregations can be easily separated from the matrix, with a significant accumulation of iron in relation to the rest of the horizon matrix, or a greater amount of iron than in the underlying rock, but they may not have enough consistency and stability to remain intact during the wetting and drying cycles. For this to occur, it seems necessary that segregations must be subjected, in the soil environment, to oxidation and reduction cycles for a sufficiently long time to acquire stability, a fact that must occur through some cementation process due to the presence of oxides and/or silica. However, it is of great value promising that the set of the three properties mentioned, plus others, should be considered in the definition of plinthite for Brazilian conditions. Some proposals in this regard are pointed out: a) that the segregations must present a greater accumulation of iron than the soil matrix and/or

than that of the underlying rock or saprolite, with the possibility of defining a minimum accumulation value (2 or 3 times greater, for example), b) that the segregations can be detached from the matrix, remaining as individualized phases, c) that they have a hard or very hard consistency when dry and a firm consistency when wet, d) that they remain sufficiently stable after several wetting cycles. For this last case, an option could be to assess its stability in water after a certain volume of the segregations is shaken in a set of sieves, defining a minimum percentage of the initial volume of material to be retained in a larger mesh sieve. Other additional criteria can be added, such as the requirement for petroplinthite in some part of the profile.

CONCLUSIONS

Genesis of high textural contrast between the horizons in soils that evolved from sedimentary rocks in the Southwest region of Rio Grande do Sul is not due only to the process of argilluviation, whereas there is strong evidence of a lithological discontinuity in some profiles, aside from ferrolysis.

X-ray diffractometry in the clay fraction and chemical analysis revealed the high levels of “exchangeable” aluminum in the Oxyaquic Hapludults, Arenic Hapludults and Oxyaquic Hapludalfs occur due to the destruction of smectite clay minerals by ferrolysis processes.

Iron segregation in most soils occurs like mottling and not plinthite, associated with iron depletion zones due to oxy-reduction reactions imposed by restrictions in water drainage in the profiles.

Despite the large number of analyses and tests used, the results showed that the identification of plinthite in soils still lacks criteria for its better characterization.

AUTHOR CONTRIBUTIONS

Conceptualization:  Pablo Grahl dos Santos (equal) and  Jaime Antonio de Almeida (equal).

Methodology:  Pablo Grahl dos Santos (lead) and  Jaime Antonio de Almeida (supporting).

Formal analysis:  Pablo Grahl dos Santos (equal) and  Jaime Antonio de Almeida (equal).

Investigation:  Pablo Grahl dos Santos (lead) and  Jaime Antonio de Almeida (lead).

Resources:  Pablo Grahl dos Santos (lead) and  Jaime Antonio de Almeida (lead).

Data curation:  Pablo Grahl dos Santos (lead) and  Jaime Antonio de Almeida (lead).

Writing - original draft:  Pablo Grahl dos Santos (equal) and  Jaime Antonio de Almeida (equal).

Writing - review and editing:  Pablo Grahl dos Santos (equal) and  Jaime Antonio de Almeida (equal).

Visualization:  Pablo Grahl dos Santos (lead).

Supervision:  Jaime Antonio de Almeida (lead).

Project administration:  Pablo Grahl dos Santos (lead).

Funding acquisition:  Jaime Antonio de Almeida (lead).

REFERENCES

- Almeida JA. Solos das pradarias mistas do sul do Brasil (Pampa Gaúcho). In: Curi N, Ker JC, Novais RF, Vidal-Torrado P, Schaefer CE, editores. *Pedologia: Solos dos biomas brasileiros*. Viçosa, MG: Sociedade Brasileira de Ciência do Solo; 2017. p. 407-66.
- Almeida JA, Klamt E, Kämpf N. Gênese do contraste textural e da degradação do horizonte B de um podzólico vermelho-amarelo da Planície Costeira do Rio Grande do Sul. *Rev Bras Cienc Solo*. 1997;21:221-33.
- Andrade H. Evolução de uma sequência de solos argilosos até arenosos no Complexo Guianense da Amazônia Ocidental [tese]. Piracicaba: Universidade do Estado de São Paulo; 1990.
- Andreis RR, Bossi GE, Montardo DK. O grupo Rosário do Sul (Triássico) no Rio Grande do Sul. In: *Anais do 31º Congresso Brasileiro de Geologia*; 1980; Camboriú, SC. Camboriú: SBG; 1980. p. 659-73.
- Bouyoucus GJ. Hydrometer method improved for making particle size analyses of soils. *Agron J*. 1962;54:464-5. <https://doi.org/10.2134/agronj1962.00021962005400050028x>
- Brasil - Ministério da Agricultura. Departamento Nacional de Pesquisa Agropecuária. Levantamento de Reconhecimento dos solos do Estado do Rio Grande do Sul. Recife: Divisão de Pesquisa Pedológica; 1973. (Boletim Técnico, 30).
- Brindley GW, Brown G. *Crystal structures of clay minerals and their X ray identification*. London: Mineralogical Society; 1980.
- Brinkman R. Ferrollysis, a hydromorphic soil forming process. *Geoderma*. 1970;3:199-206. [https://doi.org/10.1016/0016-7061\(70\)90019-4](https://doi.org/10.1016/0016-7061(70)90019-4)
- Brinkman R. Surface water gley soils in Bangladesh: genesis. *Geoderma*. 1977;17:111-44. [https://doi.org/10.1016/0016-7061\(77\)90043-X](https://doi.org/10.1016/0016-7061(77)90043-X)
- Brinkman R. Ferrollysis, a soil-forming process in hydromorphic conditions [thesis]. Wageningen: Landbouwhogeschool; 1979.
- Carvalho GBCT. Método rápido de determinação das relações Ki e Kr em solos. Rio de Janeiro: IQA; 1956. (Boletim do Instituto de Química Agrícola, 48).
- Claessen MEC. *Manual de métodos de análise de solo*. 2. ed. Rio de Janeiro: Embrapa Solos; 1997.
- Companhia de Pesquisa de Recursos Minerais - CPRM. Mapa geológico do estado do Rio Grande do Sul. Escala 1:750.000. Brasília, DF: Serviço Geológico do Brasil; 2006.
- Cunha GOM, Almeida JA, Testoni SA, Barboza BB. Formas de alumínio em solos ácidos brasileiros com teores excepcionalmente altos de Al³⁺ extraível com KCl. *Rev Bras Cienc Solo*. 2015;39:1362-77. <https://doi.org/10.1590/01000683rbc20150017>
- Espírito Santo FRC. Distribuição de óxidos de ferro em uma catena de solos derivados de granito na região fisiográfica da Depressão Central no estado do Rio Grande do Sul [dissertação]. Porto Alegre: Universidade Federal do Rio Grande do Sul; 1988.
- Holmgren GGS. A rapid citrat-dithionite extractable iron procedure. *Soil Sci Soc Am J*. 1967;31:210-1. <https://doi.org/10.2136/sssaj1967.03615995003100020020x>
- Instituto Brasileiro de Geografia e Estatística - IBGE. Levantamento de recursos naturais do projeto Radam-Brasil. Folha SH. 22 Porto Alegre e parte das folhas SH.22 Uruguaiiana e SI.22 Lagoa Mirim: geologia, geomorfologia, pedologia, vegetação, uso potencial da terra. Rio de Janeiro: IBGE; 1986.
- Instituto Brasileiro de Geografia e Estatística - IBGE. *Manual técnico de pedologia*. 3. ed. Rio de Janeiro: IBGE; 2015.
- Inda Jr AV, Kämpf N. Avaliação de procedimentos de extrações dos óxidos de ferro pedogênicos com ditionito-citrato-bicarbonato de sódio. *Rev Bras Cienc Solo*. 2003;27:1139-47. <https://doi.org/10.1590/S0100-06832003000600018>
- Jacomine PKT, Araujo Filho JC, Lima JFWF. Testes para identificação de plintita em solos da formação Solimões no Acre. In: *Anais da 9ª Reunião Brasileira de Classificação e Correlação de Solos - Solos sedimentares em sistemas amazônicos: potencialidades e demandas de pesquisa*; 2010. Rio Branco, AC. Rio Branco, AC: SBSCS; 2010. p. 27-32.

- Jimenez-Rueda JR, Demattê JLI. Solos originados de lamitos da Formação Marília (Grupo Baurú) da região de Monte Alto-SP. *Rev Bras Cienc Solo*. 1988;12:161-70.
- Justus JO, Machado MLA, Franco MSM. Geomorfologia. In: Instituto Brasileiro de Geografia e Estatística. Levantamento de Recursos Naturais. Vol. 33; Folha SH.22 Porto Alegre e parte das folhas SH.21 Uruguaiana e SI.22 Lagoa Mirim. Rio de Janeiro; 1986. p. 313-404.
- Kämpf N, Curi N. Formação e evolução do solo (Pedogênese). In: Ker JC, Curi N, Schaefer CEGR, Vidal-Torrado P, editores. *Pedologia - Fundamentos*. Viçosa, MG: Sociedade Brasileira de Ciência do Solo; 2012. p. 207-302.
- Kämpf N, Curi N. Óxidos de ferro: Indicadores de ambientes pedogênicos e geoquímicos. In: Novais RF, Alvarez VH, Schaefer CEGR, editores. *Tópicos em ciência do solo*. Viçosa, MG: Sociedade Brasileira de Ciência do Solo; 2000. v. 1. p. 81-138.
- Kehrig AG. As relações Ki e Kr no solo. Rio de Janeiro: IQA; 1949. (Boletim do Instituto de Química Agrícola, 13).
- Köppen W, Geiger R. *Klimate der Erde*. Wall-map 150 cm x 200 cm. Gotha: Verlag Justus Perthes; 1928.
- Mehra OP, Jackson ML. Iron oxide removal from soils and clays by a dithionitecitrate system buffered with sodium bicarbonate. *Clays Clay Miner*. 1960;7:317-27. <https://doi.org/10.1016/B978-0-08-009235-5.50026-7>
- Melo VF, Costa LM, Barros NF, Fontes MPF, Novais RF. Reserva mineral e caracterização mineralógica de solos do Rio Grande do Sul. *Rev Bras Cienc Solo*. 1995;19:159-64.
- Michelon CR, Azevedo AC, Pedron FA, Dalmolin RSD, Sturmmmer SK, Gonçalves J, Jesus SL. Causes of morphological discontinuities in soils of Depressão Central, Rio Grande do Sul State, Brazil. *Sci Agric*. 2010;67:319-26. <https://doi.org/10.1590/S0103-90162010000300010>
- Oliveira Junior JC, Chiapini M, Nascimento AF, Couto EG, Beirigo RM, Vidal-Torrado P. Genesis and classification of sodic soils in the northern Pantanal. *Rev Bras Cienc Solo*. 2017;41:e0170015. <https://doi.org/10.1590/18069657rbcs20170015>
- Pereira MG, Anjos LHC. Formas extraíveis de ferro em solos do estado do Rio de Janeiro. *Rev Bras Cienc Solo*. 1999;23:371-82. <https://doi.org/10.1590/S0100-06831999000200020>
- Phillips JD. Geogenesis, pedogenesis, and multiple causality in the formation of texture-contrast soil. *Catena*. 2004;58:275-95. <https://doi.org/10.1016/j.catena.2004.04.002>
- Prefeitura Municipal de Rosário do Sul - PMRS. Perfil geopolítico do município. Secretaria de Planejamento; 2005 [cited 2012 May 08]. Available from: <http://www.prefeituraderosario.com.br/planeja/planeja.htm>.
- Resende M, Curi N, Ker JC, Rezende SB. Mineralogia de solos brasileiros: interpretação e aplicações. Lavras: UFLA; 2005.
- Resende M, Santana DP. Uso das relações Ki e Kr na estimativa da mineralogia para classificação dos Latossolos. In: *Anais da 3ª Reunião de classificação, correlação dos solos e interpretação da aptidão agrícola*. Rio de Janeiro, RJ: Embrapa-SNLCS; 1988. p. 225-32.
- Santos HG, Jacomine PKT, Anjos LHC, Oliveira VA, Lumbrreras JF, Coelho MR, Almeida JA, Araújo Filho JC, Oliveira JB, Cunha TJF. *Sistema brasileiro de classificação de solos*. 5. ed. rev. ampl. Brasília, DF: Embrapa; 2018.
- Santos PG. Mineralogia, gênese e relações pedo geomórficas de solos desenvolvidos de litologias das formações Pirambóia, Sanga-do-Cabral e Guará na região sudoeste do Estado do Rio Grande do Sul [tese]. Lages: Universidade do Estado de Santa Catarina; 2015.
- Santos RD, Lemos RC, Santos HG, Ker JC, Anjos LHC. *Manual de descrição e coleta de solo no campo*. 5. ed. Viçosa, MG: Sociedade Brasileira de Ciência do Solo; 2005.
- Schaefer CER, Ker JC, Gilkes RJ, Campos JC, Da Costa LM, Saadi A. Pedogenesis on the uplands of the Diamantina Plateau, Minas Gerais, Brazil: a chemical and micropedological study. *Geoderma*. 2002;107:243-69. [https://doi.org/10.1016/S0016-7061\(01\)00151-3](https://doi.org/10.1016/S0016-7061(01)00151-3)
- Schaetzl R. Lithologic discontinuities in some soils on drumlins theory, detection, and application. *Soil Sci*. 1998;163:570-90.

- Schwertmann U, Taylor RM. Iron oxides. In: Dixon JB, Weed SB, editors. Minerals in soil environments. 2nd ed. Madison: Soil Science Society of America; 1989. p. 379-438.
- Schwertmann U. The differentiation of iron oxide in soil by a photochemical extraction with acid ammonium oxalate. *Z Pflanzenernahr Dung Bodenkd.* 1964;105:104-201.
- Soares AP, Soares PC, Holz M. Correlações Estratigráficas conflitantes no limite Permo-Triássico no Sul da Bacia do Paraná: O contato entre duas sequencias e implicações na configuração espacial do Aquífero Guarani. *Rev Pesq Geocienc.* 2008;35:115-33. <https://doi.org/10.22456/1807-9806.17942>
- Soil Survey Staff. Keys to soil taxonomy. 12th ed. Washington, DC: United States Department of Agriculture, Natural Resources Conservation Service; 2014.
- Soil Survey Staff. Soil taxonomy: a basic system of soil classification for making and interpreting soil surveys. 2nd ed. Washington, DC: United States Department of Agriculture, Natural Resources Conservation Service; 1999. (Agricultural Handbook, 436).
- Streck EV, Kämpf N, Dalmolin RSD, Klamt E, Nascimento PC, Schneider P, Giasson E, Pinto LFS. Solos do Rio Grande do Sul. 2. ed. rev. ampl. Porto Alegre: Emater; 2008.
- Tedesco MJ, Gianello C, Bissani CA, Bohnen H, Volkweiss SJ. Análises de solo, plantas e outros materiais. 2. ed. Porto Alegre: Universidade Federal do Rio Grande do Sul; 1995. (Boletim técnico, 5).
- van Reeuwijk L. Procedures for Soil Analysis. 6th ed. Wageningen: ISRIC, FAO; 2002.
- Vepraskas MJ. Redoximorphic features for identifying aquic conditions. Raleigh: North Carolina State University; 2015. (Technical Bulletin, 301).
- Whittig LD, Allardice WR. X-ray diffraction techniques. In: Klute A, editor. Methods of soil analysis. Part 1: Physical and mineralogical methods. 2nd ed. Madison: American Society of Agronomy; 1986. p. 331-62.